

Thermodynamics of Coarse Grained Models of Super-Cooled Liquids

David Chandler¹ and Juan P. Garrahan²

¹*Department of Chemistry, University of California, Berkeley, CA 94720-1460*

²*School of Physics and Astronomy, University of Nottingham, Nottingham, NG7 2RD, UK*

(Dated: March 23, 2022)

In recent papers, we have argued that kinetically constrained coarse grained models can be applied to understand dynamic properties of glass forming materials, and we have used this approach in various applications that appear to validate this view. In one such paper [J.P. Garrahan and D. Chandler, *Proc. Nat. Acad. Sci. USA* **100**, 9710 (2003)], among other things we argued that this approach also explains why the heat capacity discontinuity at the glass transition is generally larger for fragile materials than for strong materials. In the preceding article, Biroli, Bouchaud and Tarjus (BB&T) have objected to our explanation on this point, arguing that the class of models we apply is inconsistent with both the absolute size and temperature dependence of the experimental specific heat. Their argument, however, neglects parameters associated with the coarse graining. Accounting for these parameters, we show here that our treatment of dynamics is not inconsistent with heat capacity discontinuities.

I. INTRODUCTION

Many workers argue that a thermodynamic anomaly underlies the onset of glassy dynamics [1]. Evidence for this view is the rough, though not quantitative [2], correlation between dynamic fragility and excess heat capacity discontinuity [3]. This thermodynamic view contrasts with the picture we have advocated [5, 6], attributing glassy behavior to dynamic heterogeneity [4], with growing length scales appearing in space-time, but not space alone [5]. Indeed, direct observations of diffusive motion in colloidal glasses reveal excitations that are local and sparse [7]. These findings seem consistent with excitations being local and uncorrelated, as assumed in the two-state model for the low temperature behavior of structural glass heat capacities [8]. Spatial correlations under such conditions can arise through constraints on particle motions that are relieved only when adjacent regions have exhibited some degree of mobility [9, 10]. Trajectories are then correlated throughout space and time, with varying degrees of hierarchical structure determining the extent to which the system is fragile or strong [11]. From this perspective, a non-thermodynamic explanation emerges for correlation between heat capacity and fragility [12]: The concentration of excitations required to support fragile hierarchical dynamics is higher than that required for strong non-hierarchical dynamics. The juxtaposition of heat capacity discontinuities is therefore understood as a consequence of different excitation concentrations.

Biroli, Bouchaud and Tarjus (BB&T) [13] have taken issue with this explanation. They show that the simplest treatment of defect models cannot simultaneously fit the size and temperature dependence of the experimental heat capacity while simultaneously fitting dynamic properties. In general and in more current context, however, the terminology “defect models” refers to a broad class of kinetically constrained models [14]. As a result of this generality, their question “Are defect models consistent with the entropy and specific heat of glass-formers?” has a non-trivial answer (see also the analysis in [15, 16, 17]).

In particular, this class of models has an assortment of possible dynamical behaviors, so that relaxation data can be fit with many different functions of excitation concentration. In addition, kinetically constrained models are coarse grained caricatures of fluids, so that many degrees of freedom remain unspecified. Here, we focus on this latter feature, the possible consequences of unspecified degrees of freedom.

The starting point is the assumption that small length-scale and small time-scale features of a fluid can be integrated out leaving only simple stochastic rules for the dynamics of discrete variables on a lattice. These rules contain constraints imagined to be the consequence of the actual intermolecular interactions, interactions that limit the space or metric for molecular motions [18]. The excitations or defects that survive coarse graining distinguish microscopic regions of space-time that exhibit molecular mobility from those where molecules are jammed or immobile. In particular, an excitation or defect is a microscopic region of space for which particle mobility emerges. This characterization is related to coarse graining in time, because it takes time to discern whether or not mobility is exhibited. Bear in mind, “defect” does not distinguish disordered arrangements of atoms from those that are ordered because there are generally many disordered yet jammed configurations. Similarly, a lack of “excitation” does not necessarily imply low energy because some immobile regions may have the same energy as mobile regions. Uncertainty concerning this terminology may be the origin of criticisms of facilitated models leveled by BB&T [13, 19] and also by Lubchenko and Wolynes [20].

As a simple illustration, consider dividing space into cells, with grid spacing larger than the equilibrium correlation length of the material. At a given time frame, the micro states of different cells are then uncorrelated. Further, suppose there are two energy levels, 0 and J , for the states of a given cell, where the states with energy J include those that will exhibit particle mobility after a coarse graining time δt . There is a fraction, ϕ , of states with energy J that exhibit mobility in this way;

the others remain jammed. In this case the average excitation concentration is ϕ times the concentration of cells with energy J , and thus the number of molecules contributing to energy or enthalpy fluctuations is ϕ^{-1} times larger than that contributing to mobility fluctuations. In other words, when considering the thermodynamic implications of a kinetically constrained defect model, a factor ϕ^{-1} is required to account for energetic states or degrees of freedom absent from explicit consideration. BB&T ignore this factor, which leads them to the difficulties they describe.

In the next section we discuss this point in greater detail. We show that facilitated or kinetically constrained models such as the one we presented in Ref. [12] admit a variety of possibilities for partitioning micro states. This demonstration justifies the heat capacity formulas we used in Ref. [12] and therefore supports our argument about the juxtaposition of heat capacities for strong and fragile glass formers.

II. MODELS

The dynamics of facilitated models we consider are governed by master equations for distribution functions of the mobility field on a lattice. Consistent with our earlier papers, we use the symbol $n_i(t)$ to denote the value of the mobility field at lattice site i during time period t . It is a binary field in that n_i takes on one of two values, 0 (corresponding to a cell that is unexcited, jammed) or 1 (corresponding to excited, mobile). Each cell is imagined to contain several molecules, so we expect that even after some coarse graining, there are still many (not just two) microstates possible for each cell at a given time t . We further imagine these many microstates, specified with μ_i , evolve according to their own master equation. The master equation for the distribution of the mobility field n_i is a contraction of that for the micro-state field μ_i . In this section, we show how this contraction works. We begin by considering the thermodynamics and statistics of the fields n_i and μ_i , and then consider the master equations for the distributions of these fields.

A. Excitations and microstates

Imagine we partition the liquid into a lattice with grid spacing δx , and denote the state in cell i by μ_i . Imagine further that the set of available cell levels $\{\mu_i\}$ can be split into two groups: one subset of $\{\mu_i\}$ is “unexcited” with respect to mobility, $n_i = 0$, and the complementary subset is “excited”, $n_i = 1$. In practice, n_i is most conveniently determined by observing system for a coarse graining time δt . This splitting, or projection, of many micro states into two different mobility states (or several, as in the generalization of [12]) is the first central assumption of facilitated models [14].

While the state μ of a cell will correspond to one of the two mobility states, $n = 0, 1$, in general its energy, ϵ_μ , will be distributed. (For notational simplicity, when clarity is not diminished, we drop the subscripts on n_i and μ_i .) Let $G_0(\epsilon)$ and $G_1(\epsilon)$ represent the normalized probability densities for the energy levels in states $n = 0$ and $n = 1$, respectively. The cell partition function then reads (we set $k_B = 1$):

$$Z = \sum_{\mu} e^{-\epsilon_{\mu}/T} = z_0 + z_1, \quad (1)$$

where

$$z_n \equiv \omega_n \int d\epsilon G_n(\epsilon) e^{-\epsilon/T} \quad (n = 0, 1), \quad (2)$$

and ω_n gives the total number of levels in each of the two mobility states. The excitation concentration is given by:

$$c \equiv \langle n \rangle = \frac{z_1/z_0}{1 + z_1/z_0}. \quad (3)$$

The average energy per cell is:

$$\langle \epsilon \rangle = (1 - c)\langle \epsilon_0 \rangle + c\langle \epsilon_1 \rangle, \quad (4)$$

where

$$\langle \epsilon_n^k \rangle \equiv \frac{\int d\epsilon \epsilon^k G_n(\epsilon) e^{-\epsilon/T}}{\int d\epsilon G_n(\epsilon) e^{-\epsilon/T}} \quad (n = 0, 1). \quad (5)$$

The specific heat per cell is:

$$C_v = T^{-2} (\langle \epsilon_1 \rangle - \langle \epsilon_0 \rangle)^2 c(1 - c) + C_v^{(0)}(1 - c) + C_v^{(1)}c, \quad (6)$$

where

$$T^2 C_v^{(n)} \equiv \langle \epsilon_n^2 \rangle - \langle \epsilon_n \rangle^2 \quad (n = 0, 1). \quad (7)$$

The quantity $\ln(z_1/z_0)$ determines the concentration c of excitations; $\langle \epsilon_1 \rangle - \langle \epsilon_0 \rangle$ gives the average cell energy; and $T^{-2} (\langle \epsilon_1 \rangle - \langle \epsilon_0 \rangle)^2 + C_v^{(1)} - C_v^{(0)}$ sets the specific heat at small c . Except in the case where $G_n(\epsilon)$ are delta functions, these scales are in principle all different.

As a simple example, which will be useful below, consider the following model with just two energy levels. The unexcited states $n = 0$ occupy both energy levels, which we denote g and h , with energies $\epsilon_g = 0$ and $\epsilon_h = J$, respectively:

$$G_0(\epsilon) = (1 - \alpha)\delta(\epsilon) + \alpha\delta(\epsilon - J), \quad (8)$$

where α sets the relative degeneracy between the two levels. The excited states $n = 1$ have a single energy level, which we denote x , with energy $\epsilon_x = J$:

$$G_1(\epsilon) = \delta(\epsilon - J). \quad (9)$$

In this case, the cell partition function, average energy and specific heat become:

$$Z = (1 - \alpha)\omega_0 + e^{-J/T}(\alpha\omega_0 + \omega_1) \quad (10)$$

$$\langle \epsilon \rangle = J(1 - c)c_h + Jc \quad (11)$$

$$C_v = (J/T)^2 (1 - c_h)^2 c(1 - c) + (J/T)^2 c_h (1 - c_h)(1 - c), \quad (12)$$

where c_h denotes the relative occupation of the states h with respect to states g , $c_h \equiv \alpha e^{-J/T} / [(1 - \alpha) + \alpha e^{-J/T}]$. The total concentration of levels with energy J is

$$c + (1 - c)c_h \equiv \phi^{-1} c, \quad (13)$$

where we have defined ϕ as the ratio of mobile cells to the total number of cells with energy J . The specific heat then reads

$$C_v = (J/T)^2 \phi^{-1} c (1 - \phi^{-1} c). \quad (14)$$

B. Kinetics

We now show how an appropriate projection of the dynamics of the full states μ_i of individual cells into their mobility states $n_i = 0, 1$ gives a two-state facilitated model such as the FA or East models, and the slightly more general class of models introduced in Ref.[12]. The approach we take has been used to derive approximate real-space renormalization group equations [22]. Here, however, the approach requires no approximation.

The master equation for the dynamics can be written [21]:

$$\frac{\partial}{\partial t} |P(t)\rangle = -\mathcal{L} |P(t)\rangle, \quad (15)$$

where $|P(t)\rangle$ is the state vector for the probability density of the system at time t , and \mathcal{L} is the Liouvillian operator for the dynamics. In the direct product representation it reads [22]:

$$|P(t)\rangle = \sum_{\{\mu\}} P(\mu_1 \cdots \mu_N, t) |\mu_1\rangle \otimes |\mu_2\rangle \otimes \cdots \otimes |\mu_N\rangle, \quad (16)$$

where $|\mu_i\rangle$ is the state vector for level μ_i in site i .

The second assumption in facilitated models is that transitions in a cell i are only possible if neighbouring cells j are mobile, $n_j = 1$ [14]. In a system with facilitated dynamics \mathcal{L} reads [22]:

$$\mathcal{L} = \sum_i \mathcal{C}_i \ell_i \quad (17)$$

where \mathcal{C}_i is the kinetic constraint operator imposing facilitation, and ℓ_i is the unconstrained dynamic operator at site i . For example, in the East facilitated model $\mathcal{C}_i = n_{i-1}$, and in the direct product representation:

$$\mathcal{L} = \sum_i \mathbf{1} \otimes \cdots \otimes n_{i-1} \otimes \ell_i \otimes \mathbf{1} \otimes \cdots \otimes \mathbf{1}. \quad (18)$$

The off diagonal elements of ℓ_i are given by the transition rates between levels: $(\ell_i)_{\mu'\mu} = -\gamma_{\mu \rightarrow \mu'}$, while the diagonal elements are such that the sum of columns in ℓ_i vanish. A choice satisfying detailed balance is $(\ell_i)_{\mu'\mu} = -\langle \mu' | \text{eq} \rangle$, where $|\text{eq}\rangle$ is the equilibrium distribution. Notice that we have assumed that transitions between any of the levels in the cell are only possible if facilitated by a neighbour.

In order to project the dynamics of the full set of levels $|\mu\rangle$ into that of only the excitation occupancies $|n = 0, 1\rangle$ we need projection, T_1 , and embedding, T_2 , operators [22]:

$$T_1 = \sum_{n,\mu} a_{n,\mu} |n\rangle \langle \mu|, \quad T_2 = \sum_{\mu,n} b_{\mu,n} |\mu\rangle \langle n|, \quad (19)$$

where the a and b 's are constants. The projection is performed independently in each cell, so these are site diagonal operators. They must also satisfy $T_1 T_2 = \mathbf{1}$. The dynamics of the projected state $|P(t)\rangle' \equiv T_1 |P(t)\rangle$ is then given by the projected Liouvillian

$$\mathcal{L}' = T_1 \mathcal{L} T_2, \quad (20)$$

where the elements of the projection and embedding matrices (19) are given by:

$$a_{n\mu} = \delta_{n,n_\mu}, \quad b_{\mu n} = \langle \mu | \text{eq} \rangle \left(\frac{1 - n}{1 - c} + \frac{n}{c} \right) \delta_{n_\mu, n}. \quad (21)$$

The choice of rates in \mathcal{L} , which depend only on the final level, $\gamma_{\mu \rightarrow \mu'} = \langle \mu' | \text{eq} \rangle$, ensures that the projected dynamics is Markovian [23].

We now show explicitly how the projection procedure works in the simple the three-level example of the previous subsection. In this case $|\mu\rangle = |g\rangle, |h\rangle, |x\rangle$, and the onsite operators can be represented by 3×3 matrices:

$$n = \begin{pmatrix} 0 & 0 & 0 \\ 0 & 0 & 0 \\ 0 & 0 & 1 \end{pmatrix}, \quad (22)$$

$$\ell = \begin{pmatrix} c + (1 - c)c_h & -(1 - c)(1 - c_h) \\ -(1 - c)c_h & c + (1 - c)(1 - c_h) \\ -c & -c & -(1 - c)(1 - c_h) \\ & & -(1 - c)c_h \\ & & 1 - c \end{pmatrix} \quad (23)$$

Of the three levels $|\mu\rangle$, only $|x\rangle$ corresponds to the excited state, and the projection matrix is:

$$T_1 = \begin{pmatrix} 1 & 1 & 0 \\ 0 & 0 & 1 \end{pmatrix}. \quad (24)$$

The corresponding embedding matrix is:

$$T_2 = \begin{pmatrix} 1 - c_h & 0 \\ c_h & 0 \\ 0 & 1 \end{pmatrix}. \quad (25)$$

The projected operators then read:

$$n' = T_1 n T_2 = \begin{pmatrix} 0 & 0 \\ 0 & 1 \end{pmatrix}, \quad (26)$$

$$\ell' = T_1 \ell T_2 = \begin{pmatrix} c & c-1 \\ -c & 1-c \end{pmatrix}. \quad (27)$$

These are precisely the operators for a two state facilitated model [22].

III. DATA FITTING

Subsection II A tells us that if the mobility field is the result of coarse-graining and projecting the many mobile and immobile micro states, then different energy (or enthalpy) scales enter into the concentration of mobile cells c , the average energy (or enthalpy), and the specific heat. How these scales relate to each other depends on the distribution of energy levels. At equilibrium, the average excitation concentration, c , is a function of thermodynamic state. Its value should be indicative of the concentration of regions with excess energy or enthalpy, but to say more requires more assumptions or detail than needed to predict dynamical trends.

In order to illustrate how facilitated models can be used to fit thermodynamic data the simple example given above of two immobile cell levels g and h and a single mobile level x will suffice. From Eqs. (10)–(14) we see that while c gives the concentration of cells displaying mobility, both mobile and immobile cells can contribute to energy (or enthalpy) fluctuations. The relevant quantity to determine the specific heat is not c but $c + (1 - c)c_h$. From Eqs. (13) and (14) we have that the specific heat *per cell* is:

$$\begin{aligned} C_{\text{cell}} &\approx \phi^{-1} (J/T)^2 c (1 - \phi^{-1}c) \\ &\sim \phi^{-1} (J/T)^2 c, \end{aligned} \quad (28)$$

The asymptotic equality of Eq. (28) is, in effect, the expression we refer to in the penultimate paragraph of Ref. [12]. The factor ϕ^{-1} accounts for the number of molecules contributing to energy or enthalpy fluctuations, this number being larger than that for molecules contributing to mobility fluctuations. This fact is implicit in the coarse graining procedure, as shown above. In Ref. [12], ϕ^{-1} is included in the quantity we called \mathcal{N} . In the few lines devoted to this topic in Ref. [12], the meaning of \mathcal{N} was obscure and its description misleading. Indeed, where we wrote “ \mathcal{N} is the number of molecules that contribute to enthalpy fluctuations per mobile cell”, we should have written “ \mathcal{N} accounts for the number of molecules that contribute to enthalpy fluctuations beyond those associated with mobile cells.”

To be perfectly explicit, if s is the average number of molecules in a cell, then $\mathcal{N} = 1/\phi s$. With this expression, the relative values of C for several super-cooled liquids at T_g are consistent with the relative values of their heat

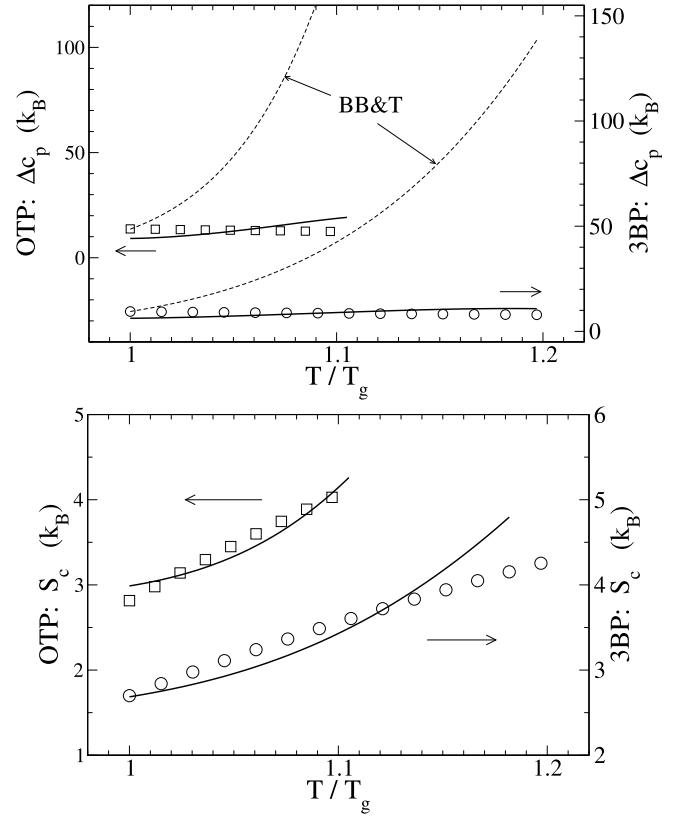


FIG. 1: Fitting of thermodynamic data near T_g using the facilitated models of Ref. [12] and compared to the formula used by Biroli, Bouchaud and Tarjus (indicated as BB&T) [13]. **Top panel:** excess specific heat, Δc_p , of supercooled OTP (left hand scale) and 3BP (right hand scale). Symbols indicate experimental data [16]. Full curves are fits using the formulas for the heat capacity per molecule discussed in the text (where $C_{\text{mol.}} \equiv \Delta c_p$): $C_{\text{mol.}} = \mathcal{N} (J/T)^2 \phi^{-1} c (1 - \phi^{-1}c)$, where $\mathcal{N} = (\phi s)^{-1}$ and $\phi = \phi_g + \phi_1 (T - T_g)/T_g$. Here $c \approx \phi e^{-J/T} \omega_1 / [(1 - \alpha)\omega_0] \approx g \exp(-J/T + J/T_{\text{ref}})$, where the first (approximate) equality neglects terms of order c^2 , and the second introduces the notation used in our Ref. [12]: g is a degeneracy that we imagine measures the possible directions of mobility, and T_{ref} bounds from above the temperatures we consider. The values of $J \approx 26.7$ and 16.7 for OTP and 3BP were determined in [12] from kinetic data. On physical grounds we expect $s \approx (J/T_m)/\Delta S_{\text{fusion}} \sim 1 - 10$, and ϕ to increase with temperature. The fitting of Δc_p gives $s, \phi_g, \phi_1 = 5, .03, .7$ and $4.5, .04, .5$ for OTP and 3BP, respectively. $\mathcal{N} \sim 6$ at T_g as argued in [12]. Clearly, it is possible to describe the size and modest change with T of the specific heat in the vicinity of T_g , in contrast to the observation of BB&T. **Bottom panel:** excess entropy, S_c , of OTP (left hand scale) and 3BP (right hand scale). Symbols correspond to experimental data [16]. Full curves are fits using the formula for the entropy per molecule which follows from Eq. (28): $S_{\text{mol.}} = s^{-1} \{ \ln[(1 - \alpha)\omega_0] - (\phi^{-1}c) \ln(\phi^{-1}c) - (1 - \phi^{-1}c) \ln(1 - \phi^{-1}c) + (\phi^{-1}c) \ln[(\omega_0\alpha + \omega_1)/(1 - \alpha)\omega_0] \}$. The shown fits correspond to the same parameters as before plus $s^{-1} \ln[(1 - \alpha)\omega_0]$, $s^{-1} \ln[(\omega_0\alpha + \omega_1)/(1 - \alpha)\omega_0] = 2.8, 1.2$ and $2.4, 1.8$ for OTP and 3BP, respectively.

capacity jumps at the glass transition. This consistency is independent of the value of s and \mathcal{N} , but the value of \mathcal{N} does play a role in the actual value of the heat capacity discontinuity. Specifically,

$$C_{\text{mol.}} \approx s^{-1} C_{\text{cell}} \approx \mathcal{N} (J/T)^2 c, \quad (29)$$

is consistent with the value of the discontinuities of the heat capacity per molecule at T_g when $\mathcal{N} \approx 6$. BB&T [13] identify s with \mathcal{N} , and further neglect the factor $1/\phi$, and in so doing disagree with this consistency.

BB&T's second criticism is about the temperature variation of C . They consider the relationship

$$C_{\text{BB\&T}} \propto (J/T)^2 c. \quad (30)$$

This formula is consistent with the asymptotic equality of Eq. (28), which requires $\phi^{-1}c$ to be small. While it is small at the glass transition, $\phi^{-1}c = sc\mathcal{N}$ may not be small at the higher temperatures considered. The right-hand side of BB&T's formula is missing the requisite factor of $(1 - \phi^{-1}c)$ present in Eq. (28). It is also missing a possible temperature dependence of ϕ . This temperature dependence would reflect that of transport in a liquid. It is typically more pronounced for isobaric temperature variation than for isochoric temperature variation, but weak and sub-Arrhenius in either case [24]. Thus, we

write $\phi \approx \phi_g + \phi_1 (T - T_g)/T_g$, where the parameters ϕ_g and ϕ_1 are temperature independent.

In Ref. [12], we chose to not consider C above T_g because doing so requires the additional parameters described in the previous paragraph. But since, BB&T raise this point, we show in Fig.1 that the effects of these extra factors on the temperature dependence of C is significant. This figure can be contrasted with that in BB&T's [13]. While the asymptotic formula predicts an exponential variation with temperature, the full formula predicts modest variation with temperature that is not inconsistent with experiment. We also show fits to the corresponding excess entropy, S_c . Better agreement between theory and experiment for these properties would require modification of the models and perhaps further parameterization.

Acknowledgments

In the US, this work was supported initially by the NSF, and more recently by DOE grant no. DE-FE-FG03-87ER13793. In the UK, it was supported by EPSRC grants no. GR/R83712/01 and GR/S54074/01, and University of Nottingham grant no. FEF 3024.

-
- [1] See, for example, D. Kivelson, S.A. Kivelson, X.-L. Zhao, Z. Nussinov, and G. Tarjus, *Physica A* **219**, 27 (1995); M. Mézard and G. Parisi, *Phys. Rev. Lett.* **82**, 747 (1999); X. Xia and P.G. Wolynes, *Proc. Natl. Acad. Sci. USA* **97**, 2990 (2000); S. Franz and G. Parisi, *J. Phys. C* **12**, 6335 (2000).
 - [2] D. Huang and G.B. McKenna, *J. Chem. Phys.* **114**, 5621 (2001); H. Tanaka, *Phys. Rev. Lett.* **90**, 055701 (2003).
 - [3] See e.g. C.A. Angell, *Science* **267**, 1924 (1995).
 - [4] For reviews see: H. Sillescu, *J. Non-Cryst. Solids* **243**, 81 (1999); M.D. Ediger, *Annu. Rev. Phys. Chem.* **51**, 99 (2000); S.C. Glotzer, *J. Non-Cryst. Solids*, **274**, 342 (2000); R. Richert, *J. Phys. Condens. Matter* **14**, R703 (2002).
 - [5] J.P. Garrahan and D. Chandler, *Phys. Rev. Lett.* **89**, 035704 (2002).
 - [6] L. Berthier and J.P. Garrahan, *Phys. Rev. E* **68**, 041201 (2003); S. Whitelam, L. Berthier and J.P. Garrahan, *Phys. Rev. Lett.* **92**, 185705 (2004); Y.J. Jung, J.P. Garrahan and D. Chandler, *Phys. Rev. E* **69**, 061205 (2004); L. Berthier, D. Chandler and J.P. Garrahan, *Europhys. Lett.* **69**, 230 (2005).
 - [7] E. Weeks, J.C. Crocker, A.C. Levitt, A. Schofield, and D.A. Weitz, *Science* **287**, 627 (2000).
 - [8] P.W. Anderson, B.I. Halperin and C. M. Varma, *Philos. Mag.* **25**, 1 (1972); W.A. Phillips, *J. Low Temp. Phys.* **7**, 351 (1972).
 - [9] S.H. Glarum, *J. Chem. Phys.* **33**, 639 (1960); M.C. Phillips, A.J. Barlow and J. Lamb, *Proc. R. Soc. Lond. A* **329**, 193 (1972).
 - [10] G.H. Fredrickson and H.C. Andersen, *Phys. Rev. Lett.* **53**, 1244 (1984).
 - [11] R.G. Palmer, D.L. Stein, E. Abrahams and P.W. Anderson, *Phys. Rev. Lett.* **53**, 958 (1984).
 - [12] J.P. Garrahan and D. Chandler, *Proc. Natl. Acad. Sci. USA* **100**, 9710 (2003).
 - [13] G. Biroli, J.-P. Bouchaud and G. Tarjus, *cond-mat/0412024* and *J. Chem. Phys.* preceding article.
 - [14] For a review see F. Ritort and P. Sollich, *Adv. Phys.* **52**, 219 (2003).
 - [15] C.A. Angell and K.J. Rao, *J. Chem. Phys.* **57**, 470 (1972).
 - [16] C.T. Moynihan and C.A. Angell, *J. Non-Cryst. Solids* **274**, 131 (2000).
 - [17] D.V. Matyushov and C.A. Angell, *cond-mat/0503082*.
 - [18] S. Whitelam and J. P. Garrahan, *J. Phys. Chem. B* **108**, 6611 (2004).
 - [19] G. Biroli and J.-P. Bouchaud, *J. Chem. Phys.* **121**, 7347 (2004).
 - [20] V. Lubchenko and P.G. Wolynes, *J. Chem. Phys.* **121**, 2852 (2004).
 - [21] E.D. Siggia, *Phys. Rev. B*, **16**, 2319 (1977).
 - [22] See, for example, S. Whitelam and J.P. Garrahan, *Phys. Rev. E* **70**, 046129 (2004).
 - [23] M. Sharpe, "General Theory of Markov Processes" (Academic Press, Boston, 1988).
 - [24] J. Jonas, *Science* **216**, 1179 (1982).